Hindawi
International Journal of Polymer Science
Volume 2017, Article ID 6792621, 9 pages
https://doi.org/10.1155/2017/6792621

Research Article

Empirical Validation of Heat Transfer Performance Simulation of Graphite/PCM Concrete Materials for Thermally Activated Building System

Jin-Hee Song,[1] Hye-Sun Jin,[1] Su-Gwang Jeong,[2] Sumin Kim,[2] Seung-Yeong Song,[1] and Jae-Han Lim[1]

[1]*Department of Architectural Engineering, Ewha Womans University, Seoul, Republic of Korea*
[2]*School of Architecture, Soongsil University, Seoul, Republic of Korea*

Correspondence should be addressed to Jae-Han Lim; limit0@ewha.ac.kr

Received 13 October 2016; Accepted 4 January 2017; Published 18 January 2017

Academic Editor: Cornelia Vasile

Copyright © 2017 Jin-Hee Song et al. This is an open access article distributed under the Creative Commons Attribution License, which permits unrestricted use, distribution, and reproduction in any medium, provided the original work is properly cited.

To increase the heat capacity in lightweight construction materials, a phase change material (PCM) can be introduced to building elements. A thermally activated building system (TABS) with graphite/PCM concrete hollow core slab is suggested as an energy-efficient technology to shift and reduce the peak thermal load in buildings. An evaluation of heat storage and dissipation characteristics of TABS in graphite/PCM concrete has been conducted using dynamic simulations, but empirical validation is necessary to acceptably predict the thermal behavior of graphite/PCM concrete. This study aimed to validate the thermal behavior of graphite/PCM concrete through a three-dimensional transient heat transfer simulation. The simulation results were compared to experimental results from previous studies of concrete and graphite/PCM concrete. The overall thermal behavior for both materials was found to be similar to experiment results. Limitations in the simulation modeling, which included determination of the indoor heat transfer coefficient, assumption of constant thermal conductivity with temperature, and assumption of specimen homogeneity, led to slight differences between the measured and simulated results.

1. Introduction

Modern lightweight construction designs, such as a curtain wall or a steel-framed structure, inevitably have less heat capacity than heavier materials. Furthermore, buildings with a high window-area ratio and internal load can create very high peak cooling loads, necessitating a technological solution to shift and reduce the peak load [1]. A thermally activated building system (TABS) is one such technologies to shift and reduce peak load. It is a radiant heating and cooling building system in which pipes embedded within the massive concrete structure supply hot and cold water [2]. Since TABS is capable of low temperature heating and high temperature cooling utilizing new and renewable energy, it is considered an energy-efficient HVAC system in green buildings.

For the application of TABS, a massive structure with high thermal inertia, such as a concrete wall or slab, is essential. Since the TABS is applied to a concrete structure with large thermal capacity, the peak heating and cooling load times can be shifted and the peak daytime load can be reduced when integrated with a traditional all-air HVAC system. However, in lightweight construction, the application of TABS is more difficult due to lack of heat capacity in the structure. To address this problem, a phase change material (PCM) can be introduced which can increase the heat capacity of lightweight construction such as deck-plate slabs, concrete hollow core slabs, or external curtain walls.

Extensive research on latent heat storage methods using PCM in buildings has been conducted [3–7]. Among the methods explored is a high-performance shape-stabilized PCM (SSPCM) that utilizes the impregnation of PCM into a porous material. In some of this research, exfoliated graphite nanoplate (xGnP) SSPCM, which performs the vacuum impregnation of a specific type of PCM into xGnP materials, is mixed with materials such as concrete and mortar [8–10].

The heat storage and dissipation characteristics of TABS using graphite/PCM concrete, which exhibit a phase change temperature, are different from TABS in conventional concrete. Therefore, different operation strategies and design guidelines for graphite/PCM concrete materials are necessary. However, not much research has been conducted on the performance of TABS applied to graphite/PCM concrete. In addition, since PCM possesses different phase change temperatures depending on type, it is important to find the most appropriate PCM for the cooling and heating in buildings. Computer simulations can effectively determine the appropriate PCM and understand its characteristics.

To evaluate the cooling and heating performance of the TABS, it is necessary to first understand various design variables such as supply and return water temperatures and heating or cooling loads. The validation of the simulation results, to verify the accurate prediction of dynamic behavior of the phase change material and its heat storage and dissipation characteristics, is necessary before these design variables are determined by simulation. In particular, as the SSPCM is mixed to concrete in the form of the graphite/PCM concrete, the validation of a simulation model with experiment results is important.

The intent of this study is to validate the simulation model for prediction of the heat storage and dissipation characteristics of the graphite/PCM concrete. For this, the simulated results were analyzed and compared to experimental data from previous study [10]. Additionally, the major contributing factors affecting performance prediction from simulation of TABS in graphite/PCM concrete, and limitations of simulation, are discussed.

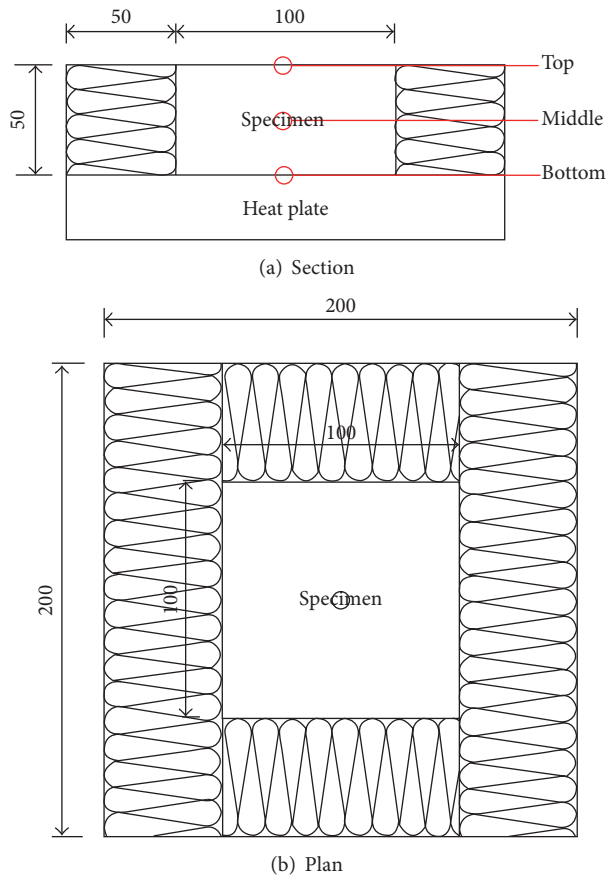

Figure 1: Specimen of the experiment.

2. Thermal Properties of Graphite/PCM

2.1. Summary of Experiment for Validation. Liquid PCM can be leaked from a building structure, owing to PCM's characteristic of solid-liquid phase change. SSPCM is a method for stabilizing the liquid PCM, which impregnates the PCM in a porous material. Various porous materials were used to make SSPCM. Kim et al. [8] proposed the n-octadecane/xGnP SSPCM and tested its thermal behavior. It can be manufactured by the vacuum impregnation of octadecane PCM in xGnP, which uses a porous nanocarbon to enhance the thermal conductivity of the PCM. In addition, Kim et al. [11] provided the appropriate mixing ratio of concrete and n-octadecane/xGnP SSPCM and tested the structural performance of concrete mixed with n-octadecane/xGnP SSPCM.

Jeong et al. [10] conducted experiments with graphite/PCM concrete, in which 100 × 100 × 50 mm cuboid specimens were made of a concrete and a graphite/PCM concrete mixed with 10 wt%, 20 wt%, and 30 wt% of SSPCM, as shown in Figure 1. Heat plates were installed under the specimen to heat it to 40, 50, and 60°C, and temperature sensors were installed at the top, middle, and bottom of each specimen.

In this study, the experimental data were obtained for the validation from the previous study [10], in which the heat plate was heated to 40°C in samples made of concrete and graphite/PCM concrete mixed with 30 wt% of SSPCM, as shown in Figure 2. The heat plate was operated in the heating mode for 4 h, followed by 20 h with the heating plate turned off and cooling down. Measured temperatures at the bottom were highest in both cases, due to proximity to the heat plate. The measured temperatures at the top location were lowest in both cases due to distance from the heating plate and heat loss to the ambient environment. In the case of the graphite/PCM concrete, temperatures were slower to both increase during the heating period and decrease during the nonheating period compared to conventional concrete.

2.2. Thermal Properties of Concrete and Graphite/PCM Concrete. The specific heat of concrete and graphite/PCM concrete is calculated from results of differential scanning calorimeter (DSC) analysis [10]. The specific heat of each concrete is shown in Figure 3. For conventional concrete, the peak point of the specific heat was not shown in the graph, indicating that concrete does not express a latent heat storage characteristic. Graphite/PCM concrete shows a rapid increase in specific heat in a temperature range between 22 and 30°C. The thermal conductivity and density of each concrete were additionally measured [10] and are shown in Table 1. The thermal conductivity was measured by using a TCi for the additional specimen of concrete with a design strength of 50 MPa. The thermal conductivity of the SSPCM itself was 1.36 W/m·K, which is less than the thermal

Table 1: Thermal conductivity and density of concrete and graphite/PCM concrete.

	Thermal conductivity	Density
Concrete	2.01 W/m·K	2.44 g/cm^3
Graphite/PCM concrete	1.60 W/m·K	2.01 g/cm^3

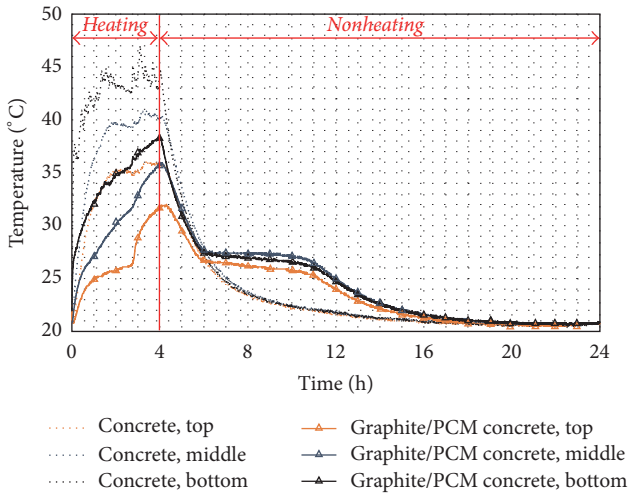

Figure 2: Experiment result of the surface and internal temperatures.

conductivity of concrete, 2.01 W/m·K. The average thermal conductivity of the graphite/PCM concrete was 1.60 W/m·K. Likewise, the density was also measured. The density of the concrete (2.44 g/cm^3) was 17.6% higher than the density of graphite/PCM concrete (2.01 g/cm^3).

3. Validation of Heat Transfer Simulation

For the steady-state simulations of TABS, ISO 11855-Part 2 Annex D [12] documents the method for verification of FEM and FDM simulation programs. In this document, the boundary conditions, material properties, and TABS model geometry are provided, and the calculated surface temperature must be within 0.3 K and the calculated heat flow within 3% of the values provided in Annex D tables for acceptable verification. Similar modeling guidelines for transient calculations of a TABS using PCM materials should be developed and verified. Therefore, in this study, comparative analysis between experimental and simulation results was conducted for the simulation model of graphite/PCM concrete with the same boundary conditions and thermal properties as the experiment. Specimens of concrete and graphite/PCM concrete as mentioned in Section 2 were modeled in Physibel Voltra 7.0w [13]. The three-dimensional transient heat transfer analysis using a finite differential method was available in this program and shown to be reliable in prior research. However, validation of the predicted thermal behavior in graphite/PCM concrete has rarely been conducted. Therefore, by comparing the simulation results

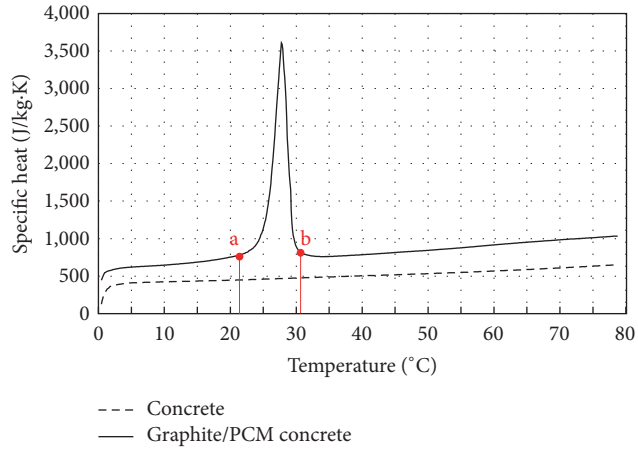

Figure 3: Specific heat of concrete and concrete with graphite/PCM.

with experimental results, the predictive capability of the simulation model for graphite/PCM concrete was assessed.

3.1. Simulation Models for Validation

3.1.1. Description of Simulation Cases. Figure 4 shows the simulation model, which is identical to the experimental specimen in Section 2. The simulation was conducted using two cases: a model of conventional concrete and one of graphite/PCM concrete. The boundary conditions of the simulation model for validation are divided into bottom, side, and top parts, as shown in Figure 4 and Table 2.

The temperature measurement points are located at the center of the top surface, the center of the bottom surface, and the internal center of the specimens (see Figure 4). The top surface temperature of the specimen was affected by the indoor temperature and convective and radiative heat transfer coefficients, while the bottom surface temperature was affected by the temperature of the heat plate and the contact thermal resistance between the specimen and the heat plate.

The temperatures used were from measured values during the experiment. The convective and radiative heat transfer coefficient of the top surface was empirically determined for more accurate surface temperatures by conducting preliminary simulations. Similarly, other preliminary simulations were conducted to determine an appropriate value for the contact thermal resistance between the specimen and the heat plate, as there is no relevant standard for this. Through the preliminary simulations, when the simulated surface temperature at the bottom point most closely approximated the temperature of the experiment, the corresponding contact thermal resistance was used. The resulting contact thermal resistances at the bottom surface of the concrete and the graphite/PCM concrete were set differently, 0.067 and 0.077 m^{2}K/W, respectively. In the experiment, the actual contact thermal resistances between each specimen and heat plate are highly likely to differ.

The thermal properties were derived from those of Section 2. The measured indoor temperatures and heat plate

Table 2: Temperature and heat transfer coefficient boundary conditions of the simulation.

Location	Boundary conditions	
	Temperature	Heat transfer coefficient/heat transfer resistance
Top surface of the model	Measured indoor air temperatures (Figure 5(a))	(a) Concrete: 7.0 W/m^{2}K (b) Graphite/PCM concrete: 7.0 W/m^{2}K
Side of the model	Adiabatic	None
Bottom surface of the model	Measured surface temperature of the heat plate (Figure 5(b))	(a) Concrete: 0.067 m^{2}K/W (b) Graphite/PCM concrete: 0.077 m^{2}K/W

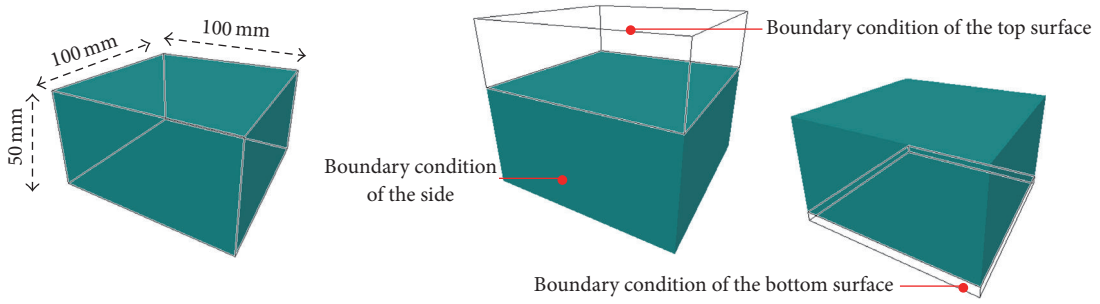

Figure 4: Simulation model.

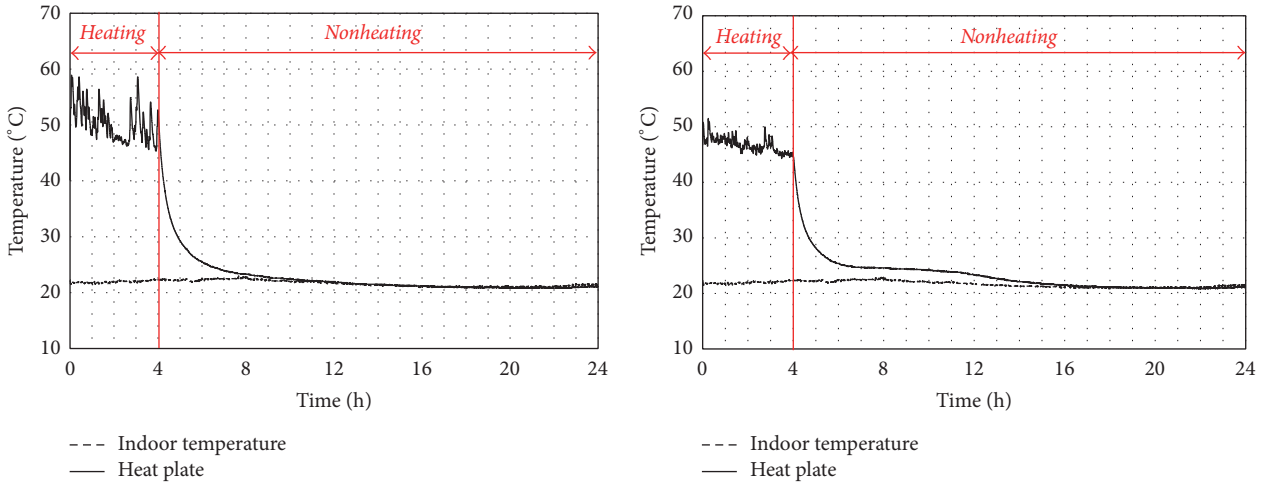

Figure 5: Heat plate and indoor temperature boundary conditions of the simulation.

temperatures were shown in Figure 5, which were used as boundary conditions. In this way, the simulation could reflect the heating and nonheating period the same as the experiment.

3.2. Comparison of Heat Transfer Characteristics. Efforts to simulate the heat storage and dissipation characteristics of the graphite/PCM concrete were focused on determining (1) whether the different thermal characteristics of concrete and graphite/PCM concrete could be predicted to agree reasonably with experiment and (2) whether the simulation could accurately predict the specific thermal characteristics resulting from the latent heat storage in the melting and freezing temperature range of the graphite/PCM concrete.

For the first assessment, a comparison of the simulated and experimental results for the top, middle, and bottom points of the concrete and graphite/PCM concrete was conducted as follows: First, the peak temperature, time to reach peak temperature at each point during the heating period, and time to reach ambient temperature during the cooling period were determined and compared. Subsequently, the mean absolute errors of the experimental and simulation results in the heating period and the nonheating period were calculated and analyzed.

For the assessment of predicted latent heat storage characteristics, the temperatures at the middle point of the graphite/PCM concrete were divided into five time zones in accordance with the melting and freezing points of the

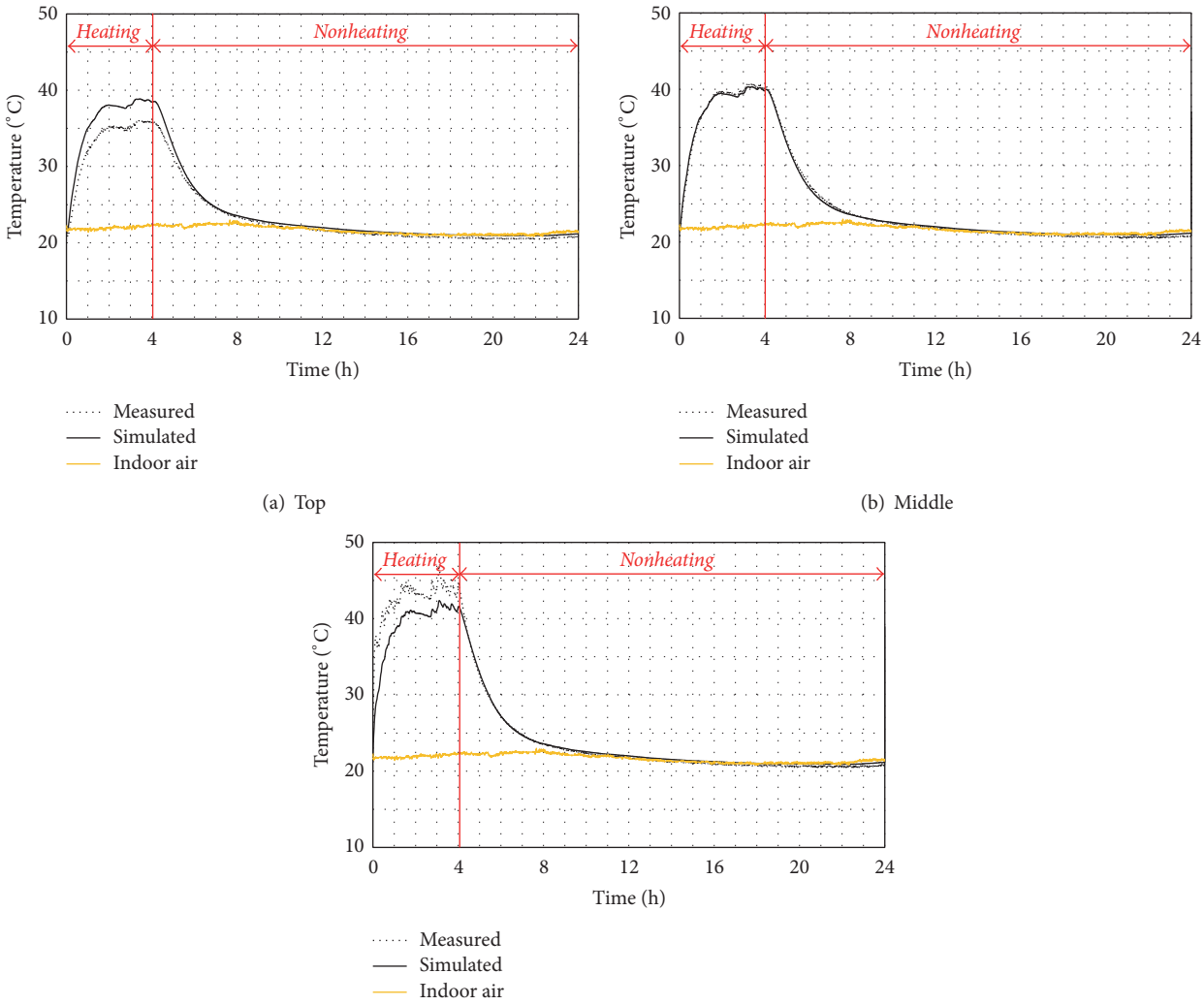

Figure 6: Temperature distributions of simulation and experimental values for concrete.

SSPCM. Subsequently, the mean absolute errors between measured and simulated values were analyzed for each of these time zones. Temperatures at the middle point were selected for analysis to minimize the influence of boundary conditions and surface thermal properties.

3.2.1. Prediction of Thermal Characteristics for Concrete and Graphite/PCM Concrete. Figures 6 and 7 show comparisons of measured and simulated temperatures at the top, middle, and bottom points of the concrete and graphite/PCM concrete specimens, respectively. In the case of the concrete in Figure 6, the temperature curves were similar at all three points. This was especially true at the middle point, while some temperatures were seen at the top and bottom points. These differences are attributed to the unknown surface thermal properties such as the convective and radiant heat transfer coefficients and the contact heat resistance. In the case of the graphite/PCM concrete in Figure 7, temperatures at the bottom and middle points showed good agreement between simulation and experiment. The temperature distribution at the middle point differed somewhat during the period of phase change, and this will be discussed later.

In both cases, the temperature distribution of the bottom point was affected by the contact thermal resistance between the specimen and the heat plate. This is an unknown for which a value must be assumed during simulation, and hence it is expected that there will be differences between the experimental and simulated values.

The simulated temperature change at the top point was different from the measured values in both cases. In particular, the graphite/PCM concrete showed a greater difference at the top compared to the two lower points. The temperature at the top point was affected by not only the phase change characteristics but also the radiant and convective heat transfer coefficients of the top surface. The radiant and convective heat transfer between the surface of a specimen and surrounding surfaces such as walls and ceilings is commonly influenced by several parameters such

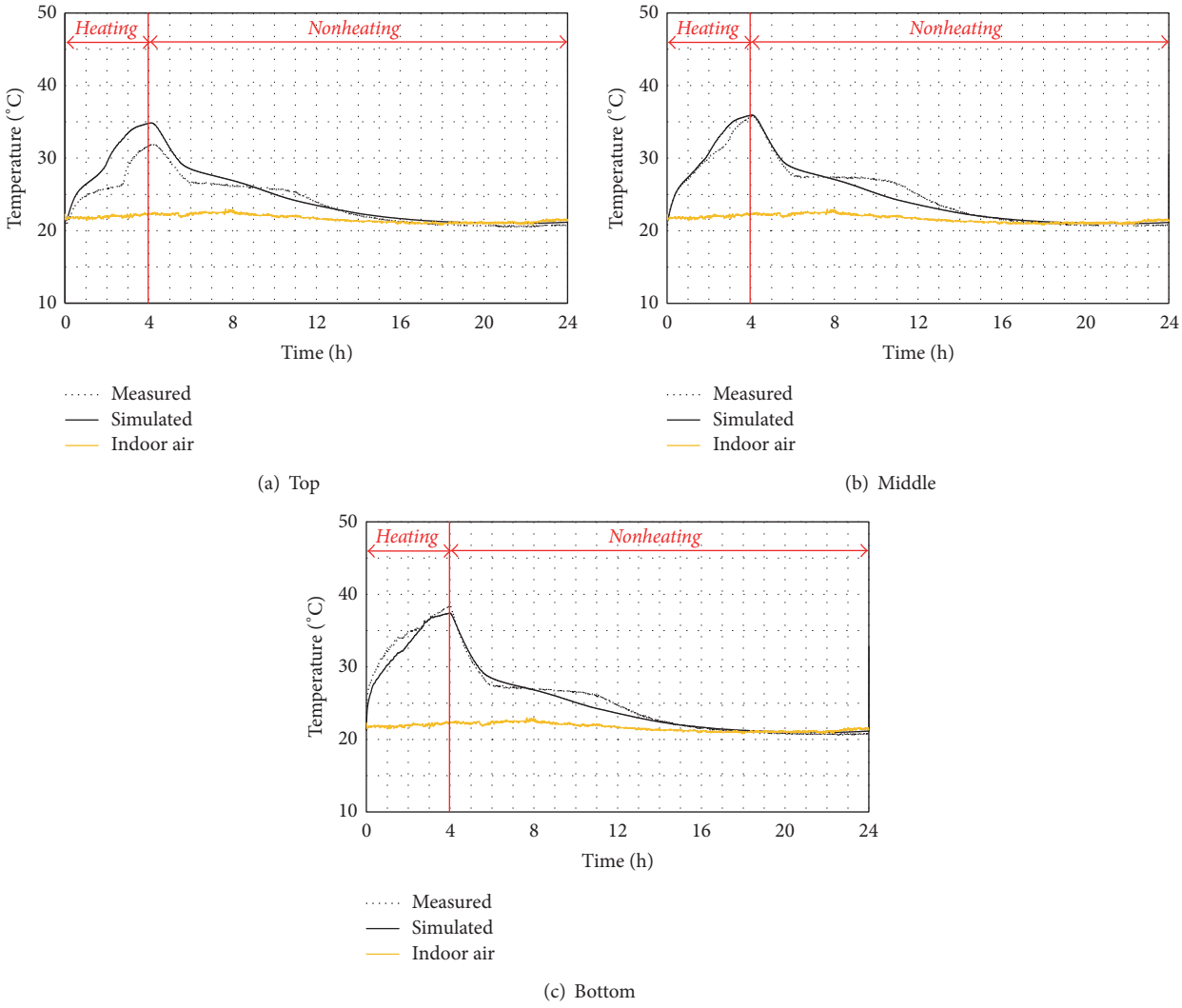

Figure 7: Temperature distributions of simulation and experimental values: concrete with graphite/PCM.

as the shape of the surroundings, interior air stratification, and air velocity. Because convective and radiant heat transfer coefficients between a heating and cooling surface and the room have different physical behaviors and are calculated with different reference temperatures, it is very important to determine an appropriate reference temperature when calculating the total heat transfer coefficient. However, during experiment or in a real building condition, the indoor surface heat transfer coefficient is difficult to measure, and design values from references such as ASHRAE [14] are often assumed. The observed top point temperature differences likely result from this assumption.

Table 3 shows peak temperatures, time to reach peak temperature, and time to arrive at the ambient temperature at each point for the two material cases. In the case of concrete, no significant difference existed between the experimental and simulated values of peak temperature at the middle point, as they differed by only 0.5°C. The peak temperatures at the top and bottom point were higher from experiment by 2.9 and 4.5°C, respectively, as the exact surface properties were difficult to obtain for simulation. Regarding the time to reach peak temperature, the simulation took 1 min longer at the lower point, 2 min longer at the middle point, and 3 min longer at the upper point when compared to experiment. Regarding the time to return to ambient temperature, the difference between the experimental and simulation values at all three points ranged from approximately 16 to 24 min to reach 22°C.

In the case of graphite/PCM concrete, an insignificant difference was seen between experimental and simulated values of peak temperature at the middle point, 0.2°C. The peak temperature at the top and bottom points was higher in experiment by 3 and 1°C, respectively. The time to reach peak temperature at all three points showed error ranging up to 2 min. Regarding the time to return to ambient temperature, there were differences of 14 to 21 min seen between the experimental and simulated values. These results indicated that simulation used can effectively predict heat storage and dissipation characteristics, except for locations affected by surface thermal properties.

Table 3: Comparison of thermal behaviors between simulation and experimental values.

Case		Peak temperature		Time to reach the peak temperature		Time to reach the ambient temperature	
		Experimental	Simulation	Experimental	Simulation	Experimental	Simulation
Concrete	Top	36.0°C	38.9°C	3.35 h	3.42 h	7.70 h	7.98 h
	Middle	40.8°C	40.3°C	3.22 h	3.18 h	8.45 h	8.05 h
	Bottom	46.9°C	42.4°C	3.08 h	3.10 h	8.88 h	9.15 h
Graphite/PCM concrete	Top	31.7°C	34.8°C	3.95 h	3.98 h	9.52 h	9.75 h
	Middle	35.7°C	35.9°C	3.97 h	3.98 h	10.23 h	9.87 h
	Bottom	38.4°C	37.4°C	3.97 h	3.97 h	10.07 h	9.83 h

Table 4: Mean absolute error between experimental and simulation values.

Case	Mean absolute error		
	Top	Middle	Bottom
Concrete			
Heating period	1.3°C	0.3°C	1.3°C
Nonheating period	0.4°C	0.3°C	0.3°C
Graphite/PCM concrete			
Heating period	3.1°C	0.7°C	1.2°C
Nonheating period	0.7°C	0.6°C	0.5°C

Table 4 shows the mean absolute errors of the experimental and simulated values at each point of the two material cases. For both cases, the temperatures at the middle point expressed similar behavior. The absolute errors were 0.3°C for both the heating and cooling periods for concrete, while for graphite/PCM concrete the mean absolute errors were 0.7 and 0.6°C for the heating and cooling periods, respectively. The mean absolute errors at the top and bottom locations during the heating period were higher than the middle, especially at the top of the graphite/PCM concrete.

3.2.2. Prediction of Thermal Characteristics due to the Latent Heat Storage for Graphite/PCM Concrete. To evaluate the predictive accuracy of heat storage and dissipation characteristics for the graphite/PCM concrete material, the simulated results were divided into five time zones, as shown in Figure 8, based on the melting and freezing temperatures range [see "a" and "b" in Figure 3]. During the heating period when the temperature of the specimen is rising, "a" in Figure 3 refers to the point at which the specific heat of the SSPCM starts to increase, the melting point, while "b" in Figure 3 refers to the point at which the specific heat returns to the normal range, the freezing point. By contrast, during the cooling period when the temperature of the specimen is decreasing, "b" in Figure 3 refers to the melting point and "a" in Figure 3 refers to the freezing point.

Table 5 shows the mean, maximum, and minimum absolute errors of each time zone. $t1$ indicates the zone from the start of the simulation to the freezing point of the SSPCM during the heating period. In good agreement with experimental values, the simulated values showed an exact prediction of the SSPCM's specific heat characteristics. The average for the experimental and simulated values was 26.6 and 26.8°C, respectively. The mean absolute error was 0.2°C,

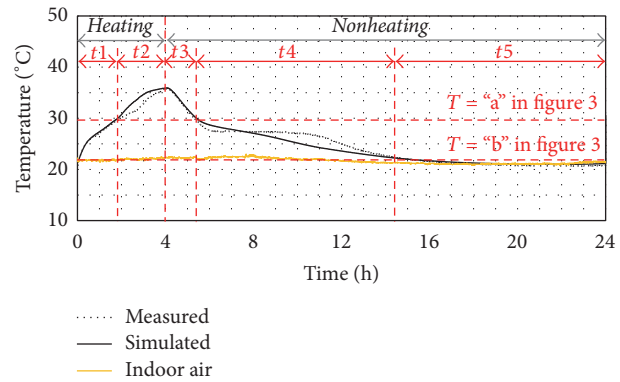

Figure 8: Detailed temperature distribution at the middle point of concrete with graphite/PCM.

which is the least of all five zones. $t2$ was started from the freezing point of the SSPCM and reached toward the end of the heating period. The experimental and simulated values have average of 32.7 and 33.9°C, respectively, with a mean absolute error of 1.2°C.

$t3$ starts at the beginning of the cooling period and ends at the melting point of the SSPCM. In this zone, the average experimental and simulated temperatures were 33.0 and 33.3°C, respectively, with a mean absolute error of 0.2°C, and similar temperature distributions are seen between the two. $t4$ starts at the melting point of the SSPCM during the cooling period and ends at the freezing point of the SSPCM. Unlike $t3$, the distribution of experimental and simulated values in $t4$ showed significant differences. The averages of the experimental and simulated values were 27.3 and 26.6°C, respectively, with an absolute error of 1.1°C. The temperature in the experiment was constantly maintained

Table 5: Average temperature and absolute error for the middle point of concrete with graphite/PCM.

Time zone	Experimental	Simulation	Absolute error (°C)		
	Average	Average	Average	Maximum	Minimum
$t1$	26.6°C	26.8°C	0.2°C	0.6°C	0.0°C
$t2$	32.7°C	33.9°C	1.2°C	2.2°C	0.2°C
$t3$	33.0°C	33.3°C	0.2°C	0.5°C	0.0°C
$t4$	27.3°C	26.6°C	1.1°C	2.4°C	0.0°C
$t5$	21.8°C	21.7°C	0.4°C	2.1°C	0.0°C

Table 6: Surface heat transfer coefficients from [2, 14, 15].

Reference	Category		Total heat transfer coefficient	
			Heating	Cooling
[2] (low temperature heating and high temperature cooling, Guidebook number 7, REHVA)	Surface type	Floor	11 W/m^{2}K	7 W/m^{2}K
		Wall	8 W/m^{2}K	8 W/m^{2}K
		Ceiling	6 W/m^{2}K	11 W/m^{2}K
[14] (ASHRAE Ch. 26 Heat, Air, and Moisture Control in Building Assemblies—Material Properties)	Direction of heat flow	Upward	9.26 W/m^{2}K	
		Horizontal	8.29 W/m^{2}K	
		Downward	6.13 W/m^{2}K	
[15] (Code for Energy-Efficient Building Design in South Korea)	Surface type	Floor/ceiling	11.63 W/m^{2}K	
		Wall	9.09 W/m^{2}K	

at approximately 27.0°C, which is the peak point of the specific heat, while the simulated temperature showed a gradual decrease within the melting and freezing range. At the conclusion of time zone $t4$, however, the temperatures had converged and hence the total dissipation times were similar. $t5$ indicates the end of the experiment, with averages of experimental and simulated values of 21.8 and 21.7°C, respectively, and a mean absolute error of 0.4°C, in good agreement.

3.3. Discussion. For the validation, it was difficult to set boundary conditions identical to the experiment for the thermal resistance of the bottom surface in contact with the heat plate and the convective and radiant heat transfer coefficient of the top surface in contact with the indoor air. As a result, the top and bottom surface temperatures showed larger differences between the experimental and simulated values than the middle point. This suggests that the surface thermal properties significantly affected the thermal behavior, and appropriate values should be determined when predicting the thermal characteristics of the TABS through a heat transfer simulation.

In a general simulation for a TABS, a convective and radiant heat transfer coefficient of heating or cooling surface is generally derived from existing references such as REHVA [2], ASHRAE [14], or a national standard [15]. These references provide the values for a heating or cooling surface as shown in Table 6.

According to Jin et al. [16], which analyzed some equations for calculating surface heat transfer coefficients, the main parameters for a convective heat transfer coefficient are indoor temperature and velocity and a shape of the surface and for a radiative heat transfer coefficient are the surface area and temperature and the averaged unheated surface temperature (AUST). For this study, the constant value, 7.0 W/m^{2}K, was used for the top surface by conducting the preliminary simulation. However, it can have limitations for the prediction of acceptable surface temperatures because the shape of the surface, the air velocity near the surface, and the averaged unheated surface temperature were not fully considered. This limitation is also shown in the heat transfer coefficient of the bottom surface. Therefore, further study should focus on determination of the proper surface thermal properties in a simulation.

The middle point did not have the influence of nearby surface thermal properties, and temperatures there were quite well predicted by the simulation. The simulated thermal characteristics of concrete were very similar to the experimental results in terms of the shape of temperature distributions. In particular, the predicted temperature at the middle point which is not affected by unknown surface thermal properties was considered as accurate, with the mean absolute error within 0.3°C. The thermal characteristics of graphite/PCM concrete were somewhat different from the experiment in the melting and freezing range of the SSPCM, with a 2.4°C maximum difference and 1.1°C mean difference.

These differences result from the thermal conductivity and density and not the specific heat. In other words, the thermal conductivity is generally entered as a constant in the simulation, regardless of the temperature, while in reality the heat conductivity varies depending on temperature. Therefore, it can be assumed that a constant thermal conductivity might have caused the observed differences in temperature distribution of the model during periods of rapid change in specific heat. Moreover, in this study, the thermal conductivity and density are measured using an additional specimen

that is different from the experimental specimens and may differ from the thermal conductivity and density of an actual specimen. Unlike the simulation model that assumed a homogeneous solid, the specimen in the experiment was made up of different and inhomogeneous materials such as gravel and sand, which might have partly affected the heat storage and dissipation characteristics. Hence, for a more accurate modeling of the SSPCM concrete in the future, the effects of the input values of heat conductivity and density on specific heat characteristics should be further analyzed.

4. Conclusions

This study aims to validate the thermal behavior of concrete mixed with SSPCM through a three-dimensional transient heat transfer simulation program. In this study, simulation models of concrete and graphite/PCM concrete were compared for prediction of the heat storage and dissipation characteristics of graphite/PCM concrete. For this, the measured and simulated results were compared and analyzed, and major factors that affect the performance prediction through the simulation of TABS in the graphite/PCM concrete and limitations of the simulation were discussed. The results of the study are as follows.

The verification results showed that the overall thermal behaviors of both the experiment and simulation of concrete and graphite/PCM concrete were similar. Especially for concrete, if boundary conditions can be matched with experiment, fairly high predictive accuracy is expected. However, at the top surface of graphite/PCM concrete, difficulty in determination of the exact indoor surface heat transfer coefficient led to larger discrepancies. Additionally, the simulated temperature distribution during the phase change period of the SSPCM also differed slightly from the experimental values, since the thermal conductivity of the graphite/PCM concrete was assumed as both homogeneous and a constant value and yet will actually depend on the material's temperature. Other causes can include differences in density and homogeneity of the specimen between the experiment and the simulation.

As a further study, a heating and cooling performance assessment for the TABS applied to graphite/PCM concrete hollow core slab will be conducted using three-dimensional heat transfer analysis. Furthermore, by conducting a sensitivity analysis regarding the major variables affecting the thermal characteristics of the graphite/PCM concrete, a modeling guideline will be provided.

Competing Interests

The authors declare that they have no competing interests.

Acknowledgments

The authors declare that there is no conflict of interests regarding the publication of this paper. This work was supported by Mid-Career Researcher Program through NRF grant funded by the MEST (no. NRF-2015R1A2A2A01004280).

References

[1] B. W. Olesen, "Using building mass to heat and cool," *ASHRAE Journal*, vol. 54, no. 2, pp. 44–52, 2012.

[2] REHVA, "REHVA Guidebook: High Temperature Cooling and Low Temperature Heating," 2010.

[3] N. Zhu, P. Hu, and L. Xu, "A simplified dynamic model of double layers shape-stabilized phase change materials wallboards," *Energy and Buildings*, vol. 67, pp. 508–516, 2013.

[4] N. Zhu, P. Liu, P. Hu, F. Liu, and Z. Jiang, "Modeling and simulation on the performance of a novel double shape-stabilized phase change materials wallboard," *Energy and Buildings*, vol. 107, pp. 181–190, 2015.

[5] A. M. Thiele, G. Sant, and L. Pilon, "Diurnal thermal analysis of microencapsulated PCM-concrete composite walls," *Energy Conversion and Management*, vol. 93, pp. 215–227, 2015.

[6] A. M. Thiele, A. Jamet, G. Sant, and L. Pilon, "Annual energy analysis of concrete containing phase change materials for building envelopes," *Energy Conversion and Management*, vol. 103, pp. 374–386, 2015.

[7] G. Zhou, Y. Yang, X. Wang, and J. Cheng, "Thermal characteristics of shape-stabilized phase change material wallboard with periodical outside temperature waves," *Applied Energy*, vol. 87, no. 8, pp. 2666–2672, 2010.

[8] S. Kim, S. J. Chang, O. Chung, S.-G. Jeong, and S. Kim, "Thermal characteristics of mortar containing hexadecane/xGnP SSPCM and energy storage behaviors of envelopes integrated with enhanced heat storage composites for energy efficient buildings," *Energy and Buildings*, vol. 70, pp. 472–479, 2014.

[9] S. Kim, S. Paek, S.-G. Jeong, J.-H. Lee, and S. Kim, "Thermal performance enhancement of mortar mixed with octadecane/xGnP SSPCM to save building energy consumption," *Solar Energy Materials and Solar Cells*, vol. 122, pp. 257–263, 2014.

[10] S.-G. Jeong, S. J. Chang, S. Wi et al., "Energy efficient concrete with n-octadecane/xGnP SSPCM for energy conservation in infrastructure," *Construction and Building Materials*, vol. 106, pp. 543–549, 2016.

[11] H. S. Kim, H. W. Min, E. M. Ryu, and A. Y. An, "Compressive strength of concrete mixed with phase change material (PCM) under thermal changes," in *Proceedings of the 22nd Annual International Conference on Composites or Nano-Engineering (ICCE '14)*, Saint Julian's, Malta, July 2014.

[12] ISO, "Building environment design—design, construction, and operation of radiant heating and cooling systems—part 2: determination of the design heating and cooling capacity," ISO 11855-2:2012, 2012.

[13] Physibel, *Physibel VOLTRA version 7.0w Manual*, 2011.

[14] ASHRAE, *ASHRAE Handbook: Fundamentals*, 2013.

[15] MOLIT, Code for Energy-efficient Building Design, South Korea: Ministry of Land, Infrastructure and Transportation, 2016.

[16] H. S. Jin, J. H. Song, J. H. Lim, S. Y. Song, and K. W. Kim, "Characteristics of convective and radiative heat transfer in the ceiling of TABS," in *Proceedings of the CLIMA 2016*, Aalborg, Denmark, May 2016.

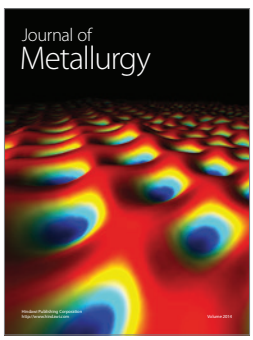

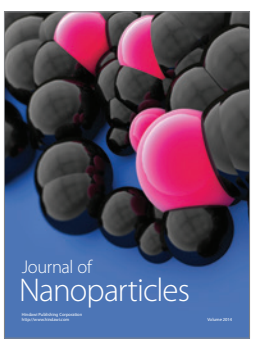

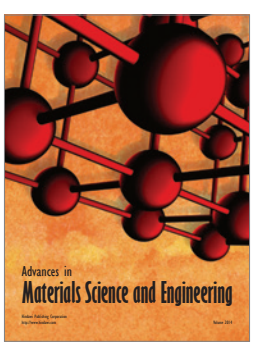

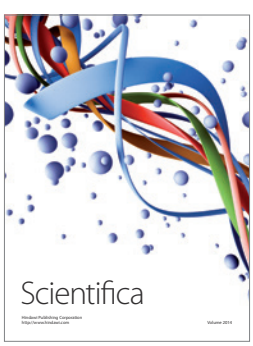

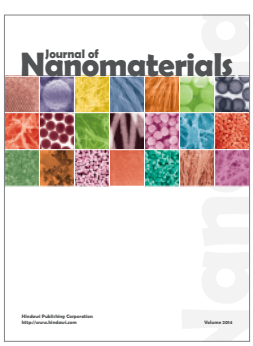

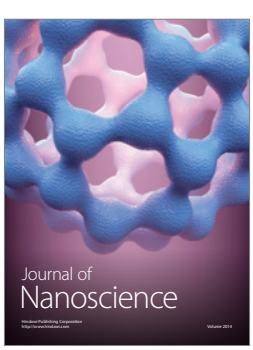

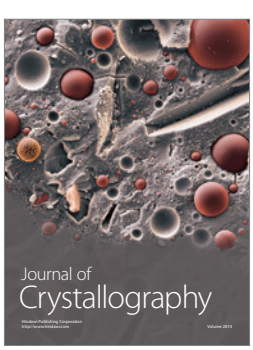

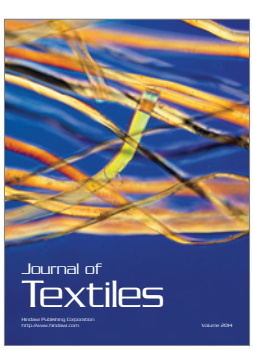

Hindawi

Submit your manuscripts at
https://www.hindawi.com